Histochem Cell Biol (2004) 122:111–119
DOI 10.1007/s00418-004-0680-2

ORIGINAL PAPER

Zhenghua Xiang · Geoffrey Burnstock

Development of nerves expressing $P2X_3$ receptors in the myenteric plexus of rat stomach

Accepted: 17 June 2004 / Published online: 16 July 2004

Abstract Development of neurones and fibres expressing $P2X_3$ receptors in the myenteric plexus of rat stomach and coexistence of the $P2X_3$ receptor with calbindin, calretinin and NOS during postnatal development, were investigated with immunostaining methods. Extrinsic nerves expressing $P2X_3$ receptors appeared as early as E12 and were localised in the trunk and branches of the vagus nerve, which extended rapidly onto the whole rat stomach from E12 to E14. Intrinsic neurone cell bodies with $P2X_3$-immunoreactivity in the myenteric ganglia were first demonstrated postnatally at P1, and at P14, when the num-ber of neurones expressing the $P2X_3$ receptor peaked at 45%. $P2X_3$ receptor-immunoreactivity decreased subsequently, and at P60 only about 11% were $P2X_3$-immunoreactive. Intraganglionic laminar nerve endings and intramuscular arrays were first demonstrated postnatally at P1 and P7, respectively. In the early postnatal days, there were many growth cone-like structures with strong $P2X_3$ immunostaining associated with these endings and arrays. Double-immunostaining showed that 9–15% of $P2X_3$-immunoreactive neurones in the gastric myenteric plexus expressed calbindin D-28 k only in the early postnatal days, while 14–21% of neurones from P1 to P60 increasingly expressed calretinin. About 20% of neurones with $P2X_3$ immunoreactivity coexpressed NOS throughout perinatal development.

Keywords $P2X_3$ receptor · Development · Stomach · Rat

Z. Xiang · G. Burnstock (✉)
Autonomic Neuroscience Institute,
Royal Free and University College London Medical School,
Rowland Hill Street, London, NW3 2PF, UK
e-mail: g.burnstock@ucl.ac.uk
Tel.: +44-20-78302948
Fax: +44-20-78302949

Z. Xiang
Department of Biochemistry and Molecular Biology,
Second Military Medical University,
200433 Shanghai, P. R. China

Introduction

The $P2X_3$ receptor is crucial, not only to peripheral sensory functions such as nociception, but also to the normal physiological regulation mediated by afferent pathways (see Burnstock and Wood 1996; Burnstock 2000, 2001). In the digestive tract, sensory nerve endings have been identified as intraganglionic laminar nerve endings (IGLEs) and intramuscular arrays (IMAs). IGLEs are specialised mechanosensory endings of vagal afferent neurones in myenteric ganglia (Powley et al. 1994; Berthoud and Neuhuber 2000; Zagorodnyuk and Brookes 2000; Zagorodnyuk et al. 2001). IGLEs are very common in the oesophageal, gastric and duodenal myenteric ganglia, and occur at lesser densities in the remaining digestive tract (Berthoud et al. 1997; Wang and Powley 2000). There has been a recent report of $P2X_2$ receptor-immunoreactivity (ir) of IGLEs in the mouse gastrointestinal tract (Castellucci et al. 2003).

Intramuscular arrays are located within the circular and longitudinal smooth muscle layers of lower oesophagus and stomach. These endings were initially described in detail by Berthoud and Powley (1992). IMAs are largely absent in the antrum, moderately dense in the corpus, and very dense in the forestomach (Phillips et al. 2000; Wang and Powley 2000). In a functional analogy with striated muscle proprioceptors, IGLEs have similarities with Golgi tendon organs, whereas IMAs have similarities with muscle spindle afferents (Phillips and Powley 2000).

In this study, we selected the stomach of rat to investigate the ontogeny and development of IGLEs, IMAs and ganglionic neurones with $P2X_3$-ir in rat stomach.

Materials and methods

Animals and tissue preparation

Breeding, maintenance and killing of the animals used in this study followed principles of good laboratory animal care and experimentation in compliance with Home Office (UK) regulations covering Schedule One Procedures and in accordance with the

Animals (Scientific Procedures) Act, 1986, governing the use of animals. All protocols were approved by the local animal ethics committee. Wistar rats of 15 different prenatal and postnatal age groups [embryonic day (E)10, E11, E12, E13, E14, E15, E16, E17, E18, E20, postnatal day (P)1, P7, P14, P30, P60] were used. Stomachs from four or five embryos from two or three rats were used for each developmental stage. Fetuses were killed by immersion in cold phosphate-buffered saline (PBS) and then fixed in 4% paraformaldehyde in 0.1 mol/l phosphate buffer, pH 7.4, while older rats were killed by asphyxiation with CO_2 and perfused through the aorta with 0.9% NaCl solution and 4% paraformaldehyde in 0.1 mol/l phosphate buffer, pH 7.4. Embryonic fetal stomachs were dissected out under a dissection microscope while the stomach of older rats was removed and washed with PBS. Stomachs of all the different ages were then refixed in 4% paraformaldehyde in 0.1 mol/l phosphate buffer, pH 7.4, overnight. The myenteric plexuses of whole-mount preparations of the stomachs from E17 to P60 were prepared under a dissection microscope. Whole-mount preparations of myenteric plexuses were not made from the stomachs of E10 to E16 fetuses; these stomachs were processed for immunostaining directly. Some of the stomachs aged from E10 to E18 were immersed in 25% sucrose PBS until they sank and then sections (10 μm) were cut from these stomachs and placed on gelatin-coated slides.

Immunocytochemistry

The development and specificity of the $P2X_3$ polyclonal antibodies has been reported previously (Xiang et al. 1998a; Oglesby et al. 1999). The immunocytochemical method was modified from our previous report (Xiang et al. 1998b). Briefly, the preparations were washed 3×5 min in 0.01 mol/l, pH 7.2, PBS and then incubated in 1.0% H_2O_2 for 30 min to block endogenous peroxidase. Preparations were preincubated in 10% normal horse serum (NHS), 0.2% Triton X-100 in PBS for 30 min, followed by incubation with $P2X_3$ antibodies, diluted 1:500 in antibody dilution solution (10% NHS, 0.2% Triton X-100 and 0.4% sodium azide in PBS) overnight at 4°C. Subsequently, preparations were incubated with biotinylated donkey anti-rabbit IgG (Jackson) diluted 1:500 in antibody dilution solution for 1 h at 37°C and then with streptavidin-HRP (Sigma) diluted 1:1,000 in PBS for 1 h at 37°C. Finally, a nickel-intensified diaminobenzidine reaction was used to visualise immunoreactivity. All incubations and reactions were separated by 3×10 min washes in PBS. The preparations were mounted, dehydrated, cleared and covered.

The following protocol was used for double immunostaining among $P2X_3$, calbindin D-28 k, calretinin, NOS and PGP9.5 (PGP9.5 was used as a general neuronal maker). The preparations were washed 3×5 min in PBS and preincubated in antibody dilution solution for 30 min, followed by incubation with $P2X_3$ antibody diluted 1:500, NOS antibody (sheep anti-rat) diluted 1:1,000, calbindin (mouse anti-rat, SWANT) diluted 1:5,000, calretinin (mouse anti-rat, SWANT) diluted 1:2,000 and PGP9.5 antibody (rabbit anti-rat) diluted 1:6,000 in antibody dilution solution overnight at 4°C. Subsequently the preparations were incubated with Cy3-conjugated donkey anti-rabbit IgG (Jackson), diluted 1:300 for P2X antibodies and FITC-conjugated donkey anti-mouse or sheep IgG (Jackson) diluted 1:200 in antibody dilution solution for calbindin, calretinin and NOS, for 1 h at room temperature. All the incubations and reactions were separated by 3×10 min washes in PBS. The preparations were evaluated with fluorescence microscopy.

Controls

Control experiments were carried out with $P2X_3$ antibodies preabsorbed with cognate peptide at a concentration of 25 μg/ml. The amino acid sequence of this peptide is VEKQSTDSGAYSIGH(383–397) (synthesised by Roche Bioscience, Palo Alto).

Photomicroscopy

Images of immunofluorescence labelling were taken with a Leica DC 200 digital camera (Leica, Switzerland) attached to a Zeiss Axioplan microscope (Zeiss, Germany). Filter sets included the following: for Cy3, excitation, 510–550 nm, emission, 590 nm; for FITC, 470 nm excitation, 525 nm emission. Images were imported into a graphics package (Adobe Photoshop 5.0, USA). The two-channel readings for green and red fluorescence were merged by using Adobe Photoshop 5.0.

Quantitative analysis

Whole-mount preparations were also used to perform a quantitative analysis, as described previously (Van Nassauw et al. 2002). Briefly, the immunoreactive-positive neurone bodies in the myenteric ganglia were counted per visual field (0.3 mm^2) in whole-mount preparations. Ten randomly chosen fields in each whole-mount preparation were studied, and the number of immunoreactive neurones was calculated.

Results

$P2X_3$-ir was first identified in the stomach of E12 fetuses. At this stage, $P2X_3$-ir was localised in the trunks of vagal nerve to stomach with short branches at the ends (Fig. 1A). At E13, the trunks of vagal nerve had more and longer branches with $P2X_3$-ir; some branches had typical $P2X_3$ receptor-labelled growth cones in the ends (Fig. 1B). About one third of the surface of the stomach was covered with $P2X_3$-immunoreactive (ir) nerve fibres at this stage. At E14, almost all of the stomach surfaces were covered with $P2X_3$-ir nerve fibres and these fibres formed networks. Only the borders of the stomach on the greater curved side were not covered with $P2X_3$-ir nerve fibres (Fig. 1D). At E15, the pattern of $P2X_3$-ir staining was similar to that at E14. At E16, the fibres formed myenteric plexus-like structures together with a few large bundles of nerve fibres with strong immunostaining (Fig. 1F). At E17, the pattern of $P2X_3$-ir was similar to that at E16. The patterns of $P2X_3$-ir at E18 and E20 were similar, but the numbers of fibres increased (Fig. 1H). In the sections of stomach at different stages, almost all $P2X_3$-ir fibres were localised in the myenteric plexus (Fig. 1C, E, G) and these $P2X_3$-ir structures were also immunoreactive for PGP9.5, a nerve fibre marker (Fig. 5K). No $P2X_3$-ir neurones or IGLE-like structures were found in embryonic stomachs.

At P1, the neurone cell bodies and IGLE-like structures with $P2X_3$-ir were first demonstrated in the myenteric plexus of the stomach, although this staining was weak to moderate. Growth cone-like structures in the myenteric plexus, where the IGLEs were forming, were prominent and these structures were usually stained strongly with $P2X_3$ antibody (Fig. 2A, B). At P7, the number and staining density of neurone cell bodies with $P2X_3$-ir increased. The number of IGLEs also increased, but the growth cone-like structures significantly decreased (Fig. 2C, D). IMA-like structures with $P2X_3$-ir were first found at this stage (Fig. 2E). At P14, the number and staining density of neurones with $P2X_3$-ir

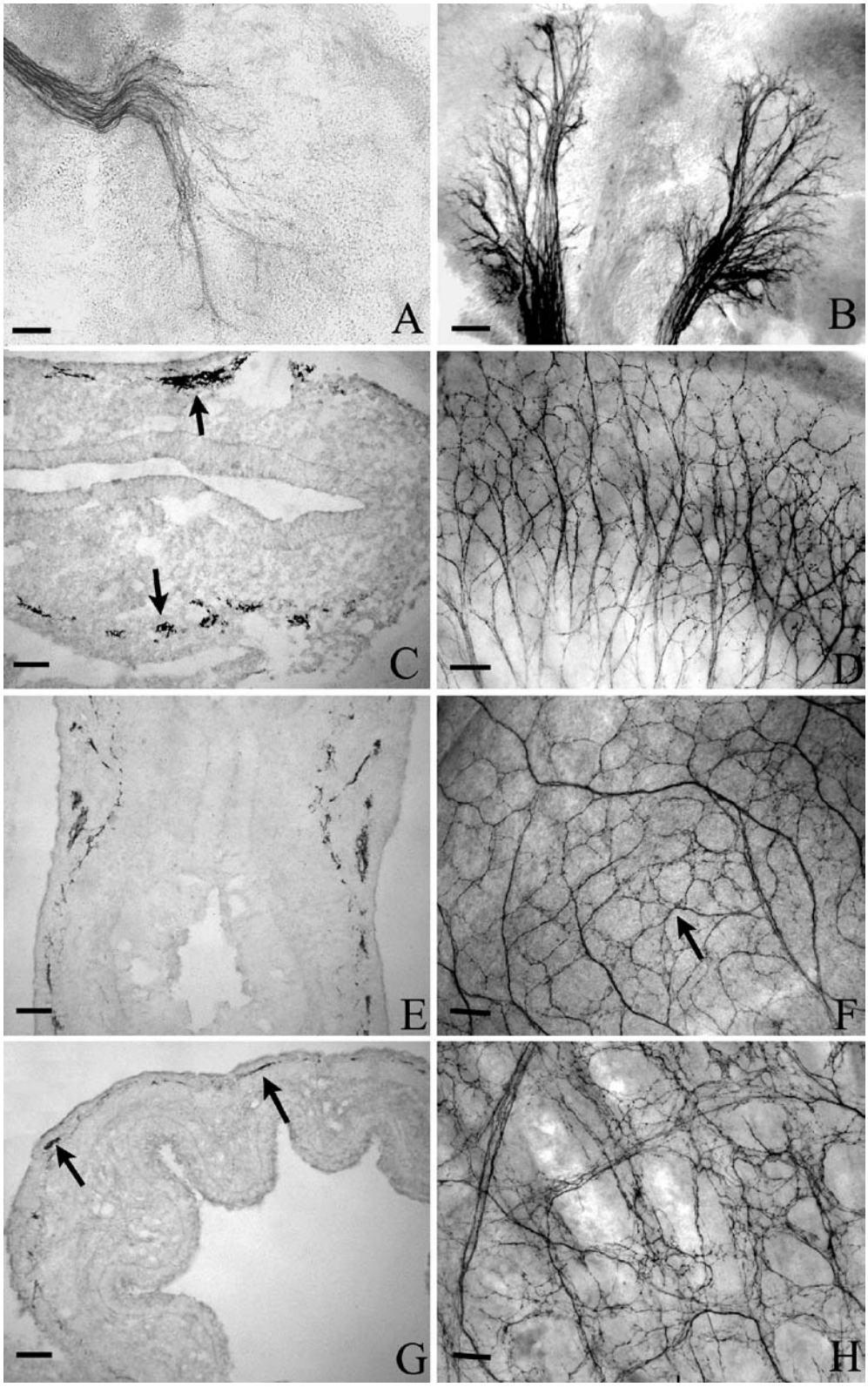

Fig. 1A–H $P2X_3$ immunoreactivity (ir) in extrinsic vagal nerve fibres in the developing rat stomach, fetal embryonic day (E)12 to E20. **A** $P2X_3$-immunoreactive (ir) vagal nerve with short branches at the ends at E12. **B** Trunks of vagal nerve and branches with $P2X_3$-ir like trees at E13. **C** Structures with $P2X_3$-ir localised between the muscular layers in rat stomach (*arrows* show positive structures). **D** At E14, almost all the surface of the stomach was covered with $P2X_3$-ir nerve fibres. **E** $P2X_3$-ir was localised between the muscular layers in rat stomach at E15. **F** $P2X_3$-ir fibres form myenteric plexus-like structures (an *arrow* shows a plexus), some nerve bundles with strong staining were scattered among the plexuses at E16. **G** $P2X_3$-ir structures were localised between muscular layers (*arrows* show positive structures) in rat stomach at E18. **H** $P2X_3$-ir structures in myenteric plexuses at E20. *Scale bars* 250 μm in **A**, **B**; 100 μm in **C–H**

continued to increase (Fig. 3A, B), and IMA-like structures expressing $P2X_3$-ir were similar to those at P7. At P30, the number of neurones in myenteric ganglia began to decrease, but the branches of IGLEs became more complex (Fig. 3C), and IMA-like structures with $P2X_3$-ir were connected to each other via networks. At P60, the number of neurones with $P2X_3$-ir in the myenteric ganglia and the morphology of IGLEs and IMAs was similar to that seen at P30 (Fig. 4A–C).

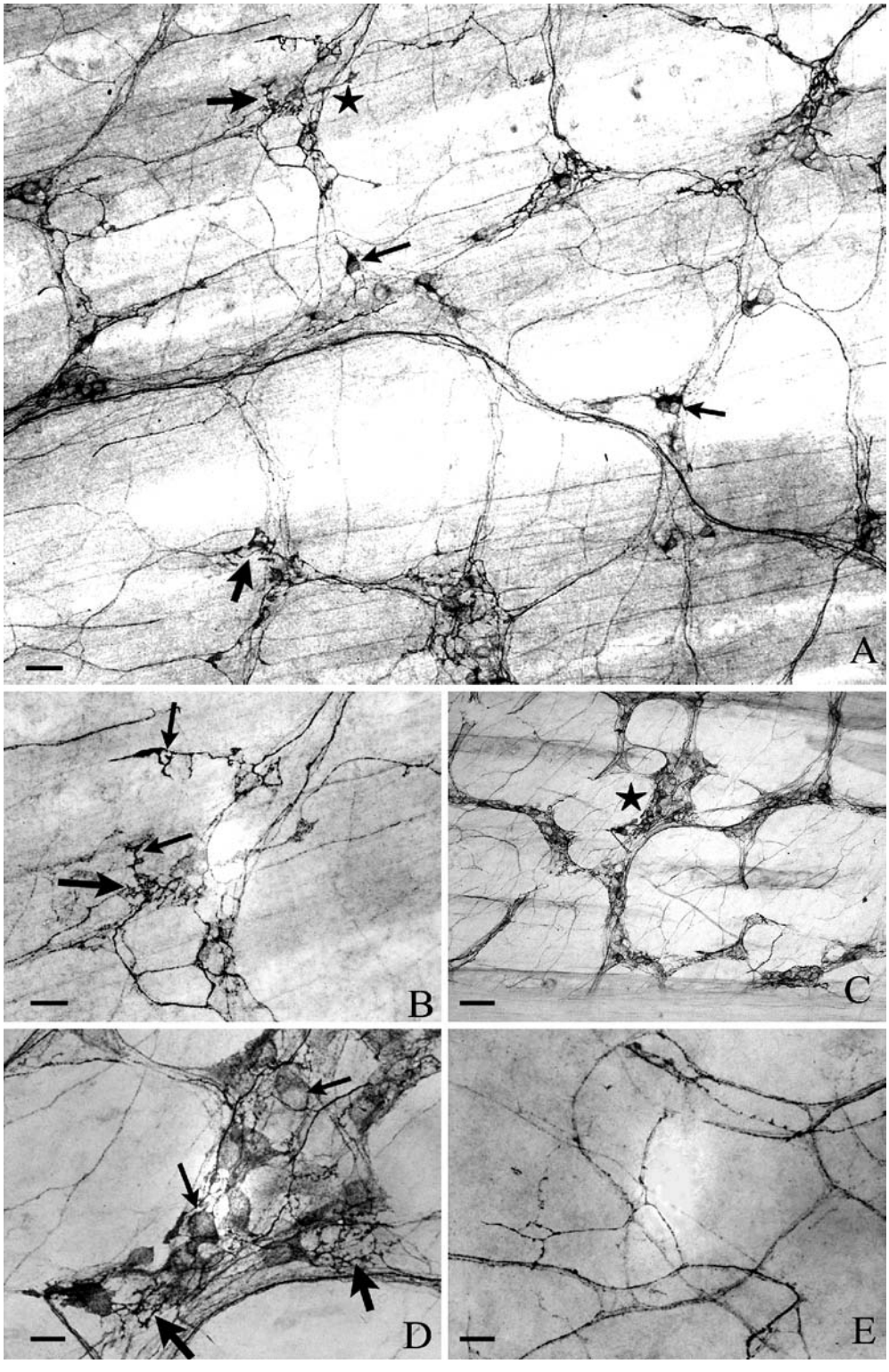

Fig. 2A–E $P2X_3$-ir in nerve cell bodies in myenteric plexus of the developing rat stomach (P1 to P7). **A** Myenteric plexuses of rat stomach with $P2X_3$-ir at P1; *thin arrows* show neurones with $P2X_3$-ir and *thick arrows* show intraganglionic laminar nerve endings (IGLEs) with $P2X_3$-ir. **B** Higher magnification of the area indicated by a *star* in **A**. **C** Myenteric plexus of rat stomach with $P2X_3$-ir at P7. **D** Higher magnification of the area indicated by a *star* in **C**. *Thin arrows* show neurones with $P2X_3$-ir and *thick arrows* show IGLEs. **E** Intramuscular arrays (IMAs) with $P2X_3$-ir at P7. *Scale bars* 80 μm in **A**; 50 μm in **B**, **E**; 100 μm in **C**; 25 μm in **D**

Double immunostaining of $P2X_3$-ir and PGP9.5-ir was used to calculate the percentages of neurones with $P2X_3$-ir in myenteric plexus of the stomach at different postnatal stages (Fig. 5L). The results are shown in Table 1. The coexistence between $P2X_3$-ir and calbindin D-28k-ir was found at P1, P7 and P14 in the myenteric plexus of rat stomach, but not at P30 and P60 (Fig. 5A–E; Table 2). The $P2X_3$-ir neurones expressing calretinin-ir or NOS-ir were found at all stages (see Fig. 5F–J; Table 2). No $P2X_3$-ir neurones were found to colocalise with substance P-ir. The IGLEs and IMA-like structures with $P2X_3$-ir were not found to be immunoreactive for calbindin D-28, calretinin, or NOS at any of the stages we examined.

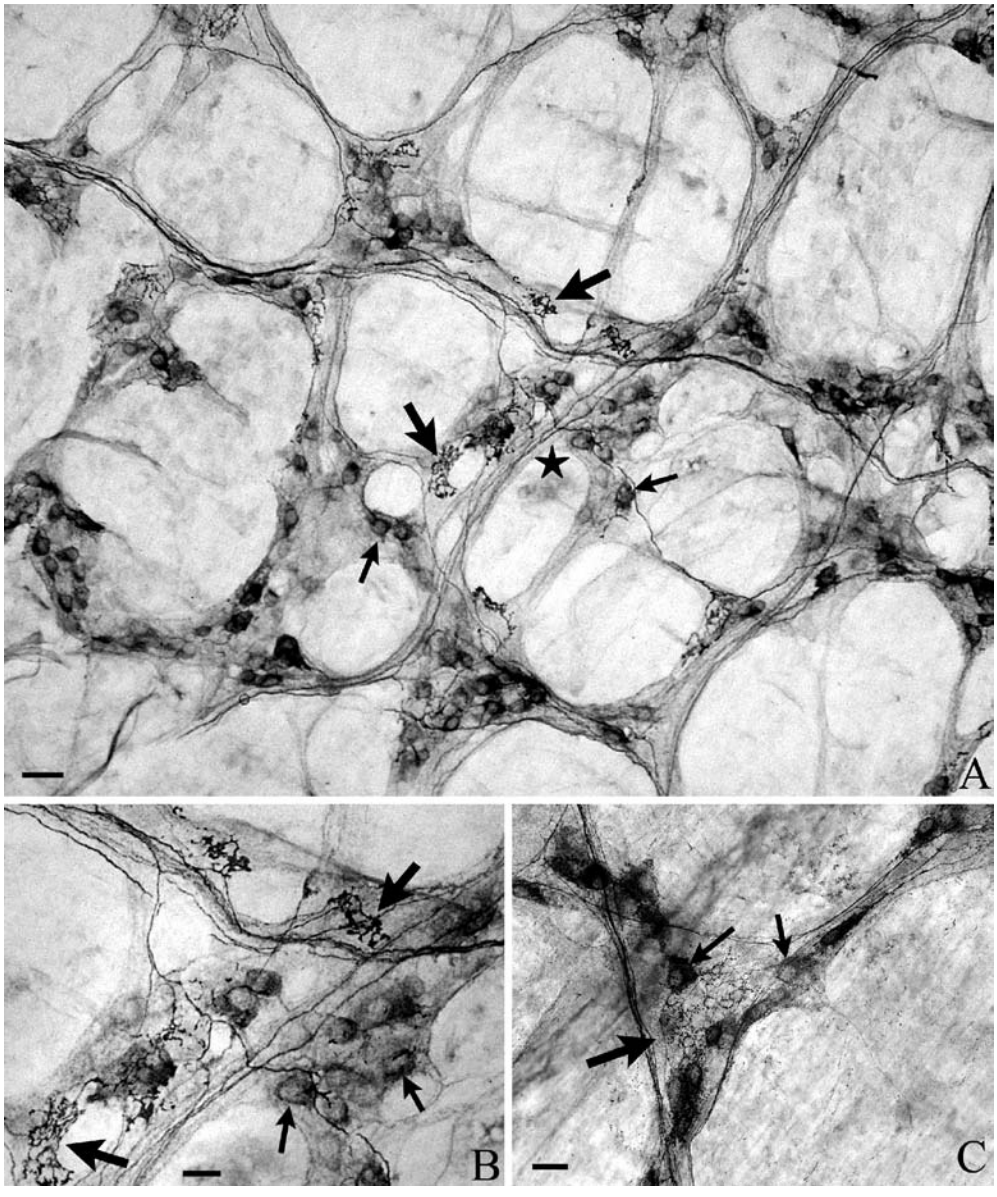

Fig. 3A–C $P2X_3$-ir in neurons and IGLEs in the developing myenteric plexus of rat stomach (P14 to P60). **A** $P2X_3$-ir structures in the myenteric plexus at P14; *thin arrows* show neurones with $P2X_3$-ir and *thick arrows* show IGLEs with $P2X_3$-ir. **B** High magnification of the area indicated by a *star* in **A**; *thin arrows* show neurones with $P2X_3$-ir and *thick arrows* show IGLEs with $P2X_3$-ir. **C** Myenteric plexus with $P2X_3$-ir at P30; *thin arrows* show neurones with $P2X_3$-ir and *thick arrow* shows IGLEs with $P2X_3$-ir. *Scale bars* 80 μm in **A**; 50 μm in **B**, **C**

Table 1 Percentages of neurone cell bodies with $P2X_3$-ir in myenteric plexuses of the rat stomach at different postnatal (*P*) stages

Stages	P1	P7	P14	P30	P60
Percentages	15±5	34±6	45±5	13±5	11±5

Table 2 Percentage of neurones with $P2X_3$-ir in myenteric plexus of the rat stomach at different postnatal (*P*) stages coexisting with calbindin (*CB*), calretinin (*CR*) and nitric oxide synthase (*NOS*)

Stages	P1	P7	P14	P30	P60
CB/$P2X_3$	11±5	9±4	15±5	0	0
$P2X_3$/CB	14±7	17±6	12±4	0	0
CR/$P2X_3$	14±5	13±4	18±7	16±5	21±6
$P2X_3$/CR	10±6	16±6	15±4	17±8	16±4
NOS/$P2X_3$	25±8	21±6	18±5	21±4	19±8
$P2X_3$/NOS	20±5	18±5	22±5	21±6	24±6

No staining was observed in those preparations incubated with the antibody solutions preabsorbed with $P2X_3$ peptides.

Discussion

The present study showed $P2X_3$-ir in both extrinsic and intrinsic enteric neurones of the rat stomach. Extrinsic nerves were seen as early as E12, localised in the vagus trunk and its branches in the rat stomach. The branches with $P2X_3$-ir extended rapidly into the whole rat stomach by E14. There were no intrinsic enteric neurone cell bodies with $P2X_3$-ir in myenteric ganglia of the embryo. The afferent neurones of vagus nerve in rat nodose ganglion were reported to express $P2X_3$ receptor at E12.5, which is consistent with the expression time of $P2X_3$-ir in

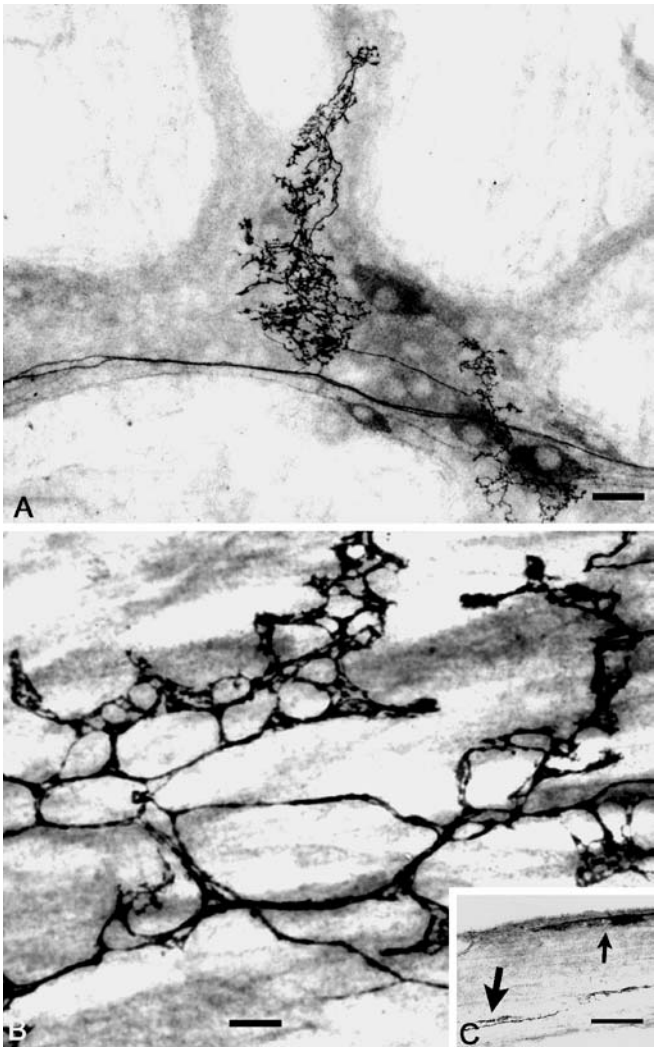

Fig. 4A–C $P2X_3$-ir neurones, IGLEs and IMAs in myenteric plexus of rat stomach at P60. **A** IGLEs and neurones with $P2X_3$-ir in myenteric plexus of rat stomach at P60. **B** IMAs with $P2X_3$-ir at P30. **C** Muscular layer section of rat stomach at P60, a *thin arrow* indicates the myenteric plexuses with $P2X_3$-ir and a *thick arrow* indicates IMAs with $P2X_3$-ir in longitudinal muscle layer. *Scale bars* 30 μm in **A**, **B**; 60 μm in **C**

rat stomach (Cheung and Burnstock 2002). The neurone cell bodies with $P2X_3$-ir in myenteric ganglia were first demonstrated in our study postnatally at P1, and at P14 the number of neurones in myenteric ganglia reached a peak, with, at that stage, about 45% neurones expressing the $P2X_3$ receptor. After this stage, the percentage of neurones expressing the $P2X_3$ receptor decreased, so that at P60 only about 11% of myenteric neurones in rat stomach were found to express the $P2X_3$ receptor. This implies that about 34% of those neurones ceased to express the $P2X_3$ receptor or died during postnatal development or that more unlabeled neurones migrated into this plexus. The second explanation seems unlikely as earlier data showed that there was no significant decrease in the total number of myenteric neurones in the rat stomach up to 2 months postnatally (Timmermans et al. 1999). The transient expression of P2X receptors has been reported during the development of other parts of the nervous system (Jarlebark et al. 2000; Nikolic et al. 2001; Cheung and Burnstock 2002). It would be very interesting to investigate the functional roles of $P2X_3$ receptors on these neurones during the periods of transient expression (from P1 to P30).

In myenteric plexus of rat stomach, IGLEs and IMAs positive for $P2X_3$ were first demonstrated at P1 and P7, respectively. We also found that in the early postnatal days (P1 and P7) growth cone-like structures with strong $P2X_3$-ir staining associated with IGLEs and IMAs were prominent. The growth cones are believed to direct neurite outgrowth by detection and response to guidance cues in the extracellular milieu (Rehder et al. 1992). They are highly dynamic and largely independent from direct control of the cell bodies. During growth cone guidance, secreted cell surface molecules bind to receptors on filopodia and lamellipodia and trigger second-messenger signals in appropriate regions of the growth cone (Schwab et al. 1993; Keynes and Cook 1995; Goodman 1996; Tessier-Lavigne and Goodman 1996). It has been suggested that ATP may regulate the morphology of the growth cones of PC12 cells induced by nerve growth factor (Schindelholz and Reber 2000). The following mechanism was proposed: that increased $[Ca^{2+}]_i$ levels activate tyrosine kinases located close to the ion channels which then leads to changes in morphology due to tyrosine phosphorylation of proteins. In the present study, we found that the growth cone-like structures in the early postnatal days (P1 to P7) showed high expression of $P2X_3$ receptors. Thus, we hypothesise that ATP may be involved in the formation of IGLEs and IMAs of the myenteric plexuses, similar to that proposed for growth cones of PC12 cells.

Fig. 5A–L Double immunostaining of $P2X_3$ receptors and calbindin, calretinin, NOS and PGP9.5 in developing myenteric plexus of rat stomach (P1 to P60). **A** Immunostaining with antibodies against $P2X_3$ (*red*). **B** Immunostaining with antibodies against calbindin D-28 k (*green*). **C** A merged image of **A** and **B** which shows some $P2X_3$-ir neurones expressing calbindin D-28 k (*yellow*) in the myenteric plexuses at P1. An *arrow* shows a double-labelled neurone. **D** Double immunolabelling of myenteric plexus at P14: $P2X_3$ immunostaining (*red*), calbindin D-28 k immunostaining (*green*), $P2X_3$-ir neurones expressing calbindin D-28 k (*yellow*). An *arrow* shows a double-labelled neurone. **E** Double immunolabelling of myenteric plexuses at P30: $P2X_3$ (*red*) and calbindin D-28 k (*green*) revealed no $P2X_3$-ir neurones expressing calbindin D-28 k. **F** Double immunostaining of myenteric plexus at P7: $P2X_3$ (*red*), calretinin (*green*), $P2X_3$-ir neurones expressing calretinin (*yellow*). An *arrow* shows a double-labelled neurone. **G** Double immunostaining of myenteric plexus at P14: $P2X_3$ (*red*), calretinin (*green*), $P2X_3$-ir neurones expressing calretinin (*yellow*). An *arrow* shows a double-labelled neurone. **H** Double immunostaining in the myenteric plexus at P30: $P2X_3$ (*red*), calretinin (*green*), $P2X_3$-ir neurones expressing calretinin (*yellow*). An *arrow* shows a double-labelled neurone. **I** Double immunostaining of the myenteric plexus at P7: $P2X_3$ (*red*) and NOS (*green*), $P2X_3$-ir neurones expressing NOS (*yellow*). An *arrow* shows a double-labelled neurone. **J** Double immunostaining of myenteric plexus at P60: $P2X_3$ (*red*), NOS (*green*), $P2X_3$-ir neurones expressing NOS (*yellow*). *Arrows* show double-labelled neurones. **K** Double immunostaining with anti-

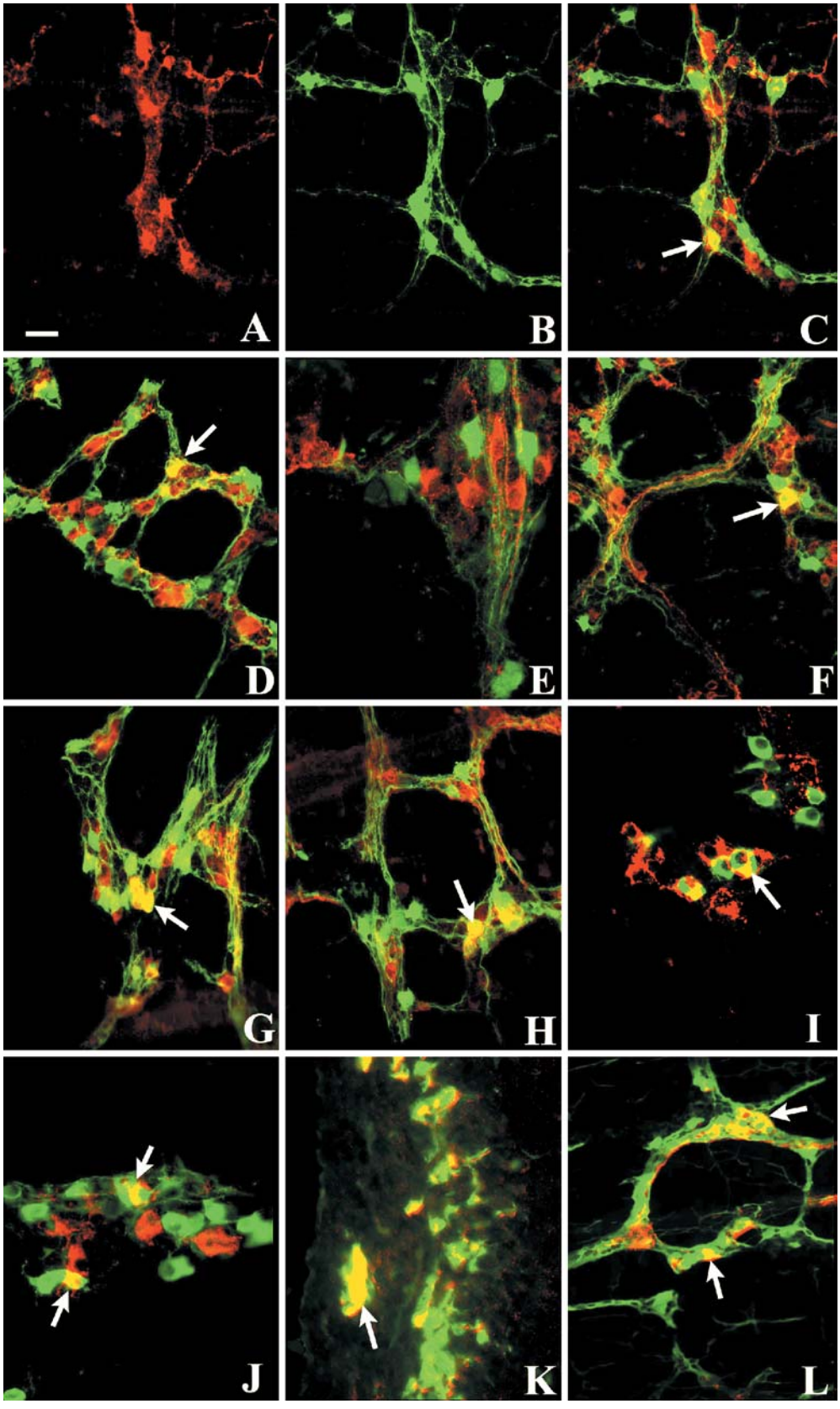

bodies against $P2X_3$ (*red*) and PGP9.5 (*green*) revealed all $P2X_3$-ir structures expressed PGP9.5 in the section of E15 rat stomach (*yellow*) but some of the structures immunoreactive for PGP9.5 did not express $P2X_3$. **L** Double immunostaining (*yellow*) with antibodies against $P2X_3$ (*red*) and PGP9.5 (*green*). *Scale bars* 75 μm in **A–L**

Intraganglionic laminar nerve endings and IMAs are believed to arise from the vagal nerve and they have been studied using anterograde tracing techniques (Clerc and Condamin 1987; Neuhuber 1987; Berthoud and Powley 1992). In the stomach, two specialised types of vagal afferent endings were distinguished within the muscularis externa using anterograde tracing techniques (Berthoud and Powley 1992). IGLEs are specialised mechanosensitive endings of vagal afferent neurones in myenteric ganglia (Berthoud and Neuhuber 2000; Zagorodnyuk and Brookes 2000). They consist of a large number of small plate-like lamellae, generally about 2–5 μm across, that interconnect with each other and form a discontinuous covering of the parts of myenteric ganglia (Neuhuber 1987). In the rat stomach, about six myenteric nerve cells are covered by each IGLE (Berthoud and Powley 1992). Recently, IGLEs have been shown to be mechanoreceptors, directly responsive to distortion with a fine probe (Zagorodnyuk and Brookes 2000). IGLEs are very common in the oesophageal, gastric and duodenal myenteric ganglia, and occur at lesser densities in the remaining digestive tract (Wang and Powley 2000). IMAs consisted of varicose nerve fibres branching and running for several millimetres parallel to bundles of longitudinal or circular muscle fibres. It has been proposed that IMAs are tension receptors. The morphology of these structures was similar to those labelled with $P2X_3$-ir in the present study and also similar to those IGLEs labelled by $P2X_2$-ir (Castellucci et al. 2003). Based on these data, $P2X_3$ purinoceptors appear likely to be involved in tension-sensory and chemosensory responses of the rat stomach. Previous data from the rat oesophagus showed colocalisation of calbindin and calretinin on IGLEs on the rat stomach (Dutsch et al. 1998). This contrasts with the present result and suggests that there are significant regional differences between the oesophagus and stomach.

In this study we showed that some of the $P2X_3$-ir neurones in the myenteric plexuses of the rat stomach expressed calbindin D-28 k in the early postnatal days, although these neurones disappeared from P30. It is believed that calbindin is a marker for intrinsic primary afferent neurones in the guinea-pig ileum (Quinson et al. 2001). In the guinea-pig ileum, $P2X_3$ receptors did not to coexpress with calbindin D-28 (Poole et al. 2002; Van Nassauw et al. 2002). In contrast, a subpopulation of myenteric neurones showed coexistence of $P2X_3$ receptors and calbindin, suggesting that it is possible that $P2X_3$ receptors are expressed on primary afferent neurones in the early postnatal days. $P2X_3$ receptors have been shown to be expressed on AH (sensory) neurones in the mouse intestine (Bian et al. 2003) and in the rat colorectum (Wynn et al. 2003). This subpopulation of myenteric neurones ceased to express $P2X_3$ receptor or calbindin from P30. So far there is no functional evidence to support the view that these myenteric neurones are primary sensory neurones. From P1 to P60, 14–21% of neurones in myenteric plexus of rat stomach coexpressed calretinin. This compares to about 80% of the neurones coexpressing calretinin and $P2X_3$-ir in myenteric plexus of rat small intestine and colon (Xiang and Burnstock 2004). Coexistence of $P2X_3$ receptors and calretinin in the myenteric plexus of the stomach was also seen but at a lower level than in the intestine. Calretinin is believed to be a marker for cholinergic secretomotor and vasomotor neurones (Li and Furness 1998). This suggests that there are fewer cholinergic neurones in the myenteric plexus of rat stomach compared to small intestine and colon. The percentage of neurones where $P2X_3$-ir coexists with NOS did not change significantly during development, consistent with that found for the myenteric plexus of the guinea-pig (Van Nassauw et al. 2002).

In summary, $P2X_3$-ir of nerves in the rat stomach is composed of two types: extrinsic and intrinsic. The extrinsic nerve fibres were first seen as early as E12 and extended rapidly onto the whole rat stomach from E12 to E14. The enteric neurone cell bodies in the myenteric plexus with $P2X_3$-ir were first demonstrated at P1; at P14 the number of neurone cell bodies with $P2X_3$-ir reached a peak with about 45% of the neurones expressing $P2X_3$ receptors. After this stage, the percentage of neurones expressing $P2X_3$ receptors decreased to about 11% at P60. $P2X_3$ receptor-labelled IGLEs and IMAs were first demonstrated at P1 and P7, respectively. In the early postnatal days there were many growth cone-like structures with strong $P2X_3$-ir staining associated with IGLEs and IMAs. Double immunostaining showed 9–15% of $P2X_3$-ir neurones in the myenteric plexuses expressed calbindin D-28 k in the early postnatal days. From P1 to P60, 14–21% of neurones in the stomach expressed calretinin, but in the rat colon and small intestine the percentage was considerably higher (Xiang and Burnstock 2004). The percentage of neurones with $P2X_3$-ir coexisting with NOS did not change significantly during perinatal development.

Acknowledgements The authors thank Dr. Chrystalla Orphanides for editorial assistance.

References

Berthoud HR, Neuhuber WL (2000) Functional and chemical anatomy of the afferent vagal system. Auton Neurosci 85:1–17

Berthoud HR, Powley T (1992) Vagal afferent innervation of the rat fundic stomach: morphological characterization of the gastric tension receptor. J Comp Neurol 319:261–276

Berthoud HR, Patterson LM, Neumann F, Neuhuber WL (1997) Distribution and structure of vagal afferent intraganglionic laminar ending IGLEs in the rat gastrointestinal tract. Anat Embryol 195:183–191

Bian X, Ren J, De Vries M, Schnegelsberg B, Cockayne DA, Ford APDW, Galligan JJ (2003) Peristalsis is impaired in the small intestine of mice lacking the $P2X_3$ subunit. J Physiol 551:309–322

Burnstock G (2000) P2X receptors in sensory neurones. Br J Anaesth 84:476–488

Burnstock G (2001) Purine-mediated signaling in pain and visceral perception. Trends Pharmacol Sci 22:182–188

Burnstock G, Wood JN (1996) Purinergic receptors: their role in nociception and primary afferent neurotransmission. Curr Opin Neurobiol 6:526–532

Castellucci P, Robbins HL, Furness JB (2003) P2X(2) purine receptor immunoreactivity of intraganglionic laminar endings in the mouse gastrointestinal tract. Cell Tissue Res 312:167–174

Cheung KK, Burnstock G (2002) Localization of $P2X_3$ receptors and coexpression with $P2X_2$ receptors during rat embryonic neurogenesis. J Comp Neurol 443:368–382

Clerc N, Condamin M (1987) Selective labeling of vagal sensory nerve fibers in the lower esophageal sphincter with anterogradely transported WGA-HRP. Brain Res 424:216–224

Dutsch M, Eichhom U, Worl J, Wank M, Berthound HR, Neububer WL(1998) Vagal and spinal afferent innervation of the rat esophagus: a combined retrograde tracing and immunocytochemical study with special emphasis on calcium-binding proteins. J Comp Neurol 398:289–307

Goodman CS (1996) Mechanisms and molecules that control growth cone guidance. Annu Rev Neurosci 19:341–377

Jarlebark LE, Housley GD, Thorne PR (2000) Immunohistochemical localization of adenosine 5′-triphosphate-gated ion channel P2X(2) receptor subunits in adult and developing rat cochlea. J Comp Neurol 421:289–301

Keynes RJ, Cook GMW (1995) Repulsive and inhibitory signals. Curr Opin Neurobiol 5:75–82

Li ZS, Furness JB (1998) Immunohistochemical localization of cholinergic markers in putative intrinsic primary afferent neurones of the guinea-pig small intestine. Cell Tissue Res 204:35–43

Neuhuber WL (1987) Sensory vagal innervation of the rat esophagus and cardia: a light and electron microscopic anterograde tracing study. J Auton Nerv Syst 20:243–255

Nikolic P, Housley GD, Luo L, Ryan AF, Thorne PR (2001) Transient expression of P2X(1) receptor subunits of ATP-gated ion channels in the developing rat cochlea. Brain Res Dev Brain Res 126:173–182

Oglesby IB, Lachnit WG, Burnstock G, Ford APDW (1999) Subunit specificity of polyclonal antisera to the carboxy terminal regions of P2X receptors $P2X_1$ through $P2X_7$. Drug Dev Res 47:189–195

Phillips RJ, Powley TL (2000) Tension and stretch receptors in gastrointestinal smooth muscle: re-evaluating vagal mechanoreceptor electrophysiology. Brain Res Revs 34:1–26

Phillips RJ, Baronowsky EA, Powley TL (2000) Regenerating vagal afferents reinnervate gastrointestinal tract smooth muscle of the rat. J Comp Neurol 421:325–346

Poole DP, Castelucci P, Robbins HL, Chiocchetti R, Furness JB (2002) The distribution of $P2X_3$ purine receptor subunits in the guinea pig enteric nervous system. Auton Neurosci 101:39–47

Powley TL, Holst MC, Boyd DB, Kelly JB (1994) Three-dimensional reconstructions of autonomic projections to the gastrointestinal tract. Microsc Res Tech 29:297–309

Quinson N, Robbins HL, Clark MJ, Furness JB (2001) Calbindin immunoreactivity of enteric neurones in the guinea-pig ileum. Cell Tissue Res 305:3–9

Rehder V, Jensen JR, Kater SB (1992) The initial stages of neural regeneration are dependent upon intracellular calcium levels. Neuroscience 51:565–574

Schindelholz B, Reber BF (2000) L-type Ca^{2+} channels and purinergic $P2X_2$ cation channels participate in calcium-tyrosine kinase-mediated PC12 growth cone arrest. Eur J Neurosci 12:194–204

Schwab ME, Kapfhammer JP, Bandtlow CE (1993) Inhibitors of neurite growth. Annu Rev Neurosci 16:565–595

Tessier-Lavigne M, Goodman CS (1996) The molecular biology of axon guidance. Science 274:1123–1133

Timmermans JP, Adriaensen D, Lefebvre R (1999) Postnatal development of nitrergic neurons in the myenteric plexus of rat stomach. Histochem Cell Biol 111:429–434

Van Nassauw L, Brouns I, Adriaensen D, Burnstock G, Timmermans JP (2002) Neurochemical identification of enteric neurones expressing $P2X_3$ receptors in the guinea-pig ileum. Histochem Cell Biol 118:193–203

Wang FB, Powley TL (2000) Topographic inventories of vagal afferents in gastrointestinal muscle. J Comp Neurol 421:302–324

Wynn G, Rong W, Xiang Z, Burnstock G (2003) Purinergic mechanisms contribute to mechanosensory transduction in the rat colorectum. Gastroenterology 125:1398–1409

Xiang Z, Burnstock G (2004) $P2X_2$ and $P2X_3$ purinoceptors in the rat enteric nervous system. Histochem Cell Biol 121:169–179

Xiang Z, Bo X, Burnstock G (1998a) Localization of ATP-gated P2X receptor immunoreactivity in rat sensory and sympathetic ganglia. Neurosci Lett 256:105–108

Xiang Z, Bo X, Oglesby IB, Ford APWD, Burnstock G (1998b) Localization of ATP-gated $P2X_2$ receptor immunoreactivity in the rat hypothalamus. Brain Res 813:390–397

Zagorodnyuk VP, Brookes SJH (2000) Transduction sites of vagal mechanoreceptors in the guinea pig esophagus. J Neurosci 20:249–255

Zagorodnyuk VP, Chen BN, Brookes SJH (2001) Intraganglionic laminar endings are mechano-transduction sites of vagal tension receptors in the guinea pig stomach. J Physiol 534:255–268